

Setting Reference Level in the Human Safety Guidelines via Nerve Activation Intercomparison

Jose Gomez-Tames
Essam Rashed
Akimasa Hirata

Department of Electrical and Mechanical Engineering
Nagoya Institute of Technology
Nagoya, Japan

Thomas Tarnaud
Emmeric Tanghe
Tom Van de Steene
Luc Martens
Wout Joseph

Department of Information Technology
Ghent University/IMEC
Ghent, Belgium

Abstract—International guidelines/standards have been published for human protection from electromagnetic field exposure. The research in the intermediate frequencies is scattered unlike for other frequencies, and thus the limit prescribed in the guidelines/standards are different by a factor of 10. The IEEE International Committee on Electromagnetic Safety has published a research agenda for exploring the electrostimulation thresholds. However, the consistency of the excitation models for specific target tissue needs to be revised. For this purpose, we present the first intercomparison study using multiphysics modelling to investigate stimulation thresholds during transcranial magnetic stimulation (TMS). To define the stimulation threshold, a non-invasive technique for brain stimulation has been used. In this study, by incorporating individual neurons into electromagnetic computation in realistic head models, stimulation thresholds can be determined. Then, we demonstrated that the allowable external magnetic field strength in the current guidelines/standard is conservative.

Keywords—Stimulation threshold; TMS; Electric Field; Nerve Model; Intercomparison; Multiphysics; Dosimetry;

I. INTRODUCTION

There have been concerns about potential adverse health effects caused by human exposure to electromagnetic fields. For human exposure to electromagnetic fields, the dominant biological effect is electrostimulation at frequencies typically lower than 100 kHz, while and thermal effect is described at the frequencies higher than 100 kHz in the international standards/guidelines [1], [2]. In the standards/guidelines, the safety/reduction factor is applied to known or operational thresholds. However, in the intermediate frequencies where the stimulation is attributable to the axon activation, the threshold assessment for the pain or sensory effect is limited.

To derive a limit in a scientific manner combining the electromagnetics and neuron model is listed in the research agenda of the IEEE International Committee on Electromagnetic Safety (ICES) [3]. A working group on ‘Exploring the electrostimulation threshold in the brain’ has been established in IEEE ICES to clarify certain aspects, and is led by the authors. The mission of this working group includes

assessment of brain stimulation threshold variability by combined modelling of electromagnetics and CNS neuron models.

However, due to ethical problems, it is difficult to evaluate the human threshold of stimulation in non-medical applications. Stimulation thresholds can be determined by transcranial magnetic stimulation (TMS), which is a non-invasive brain stimulation technique. TMS induces an eddy current in the brain to activate a target area when a strong pulsed current is injected into a coil. The most common protocol for TMS is targeting the motor cortex owing to the presence of a relatively straightforward measurable marker of activation, such as the threshold for motor evoked potentials (MEPs). The threshold for MEPs is used in the clinical application as a percentage of the maximum stimulation output of the stimulation device. However, the *in-situ* electric field for stimulation threshold in the brain are unknown from *in vivo* human measurements.

Computational models thus have been used to determine the *in-situ* electric fields (EFs). Computational dosimetry becomes an essential tool for estimating induced physical quantities. Some of the techniques have been developed for human safety, and now it has also been extended to medical applications, including diagnoses, treatment of diseases, and investigating human brain functions *in vivo* [4]. There is an increasing trend in incorporating individual neurons into realistic head models that can be used to investigate neuron stimulation thresholds. However, the consistency of excitation models for a specific target tissue needs to be revised.

In this study, an intercomparison of the EF computation and its effects using nerve modelling has been conducted for the first time. Different numerical methods were used to compute the EF and axon model to account for model differences. Then, the reference levels, which are the allowable field strengths in the international guidelines/standard, have been derived to discuss their conservativeness in the guidelines.

II. MODEL AND METHODS

A. Human Models and Exposure Scenarios

We used a freely available magnetic resonance image database to create a realistic head model (available on <http://hdl.handle.net/1926/1687>). The head model consisted of 14 tissues/body fluids, of which the electrical conductivities were determined using the fourth order Cole-Cole model [5] at 10 kHz. The model resolution was 0.5 mm (65.3×10^6 voxels). Tissue conductivity was assumed to be linear and isotropic.

A figure-eight coil was modeled as a single loop of thin wire with a radius for each winding of 70 mm in diameter and an input current of 1 A. The position of the coil was over the midline central position (CZ position in the 10-20 system) with a medial-lateral orientation of the coil in subsection III.A of this paper. The coil was configured to stimulate the motor cortex in subsection III.B. The optimal coil orientation was along the anterior-posterior orientation (well-known orientation for the motor cortex). The stimulation position on the scalp was optimized for maximum EF strength in the hand motor cortex. The reference level was derived using a uniform low-frequency exposure (1, 10, and 100 kHz) in the lateral-medial direction to activate the pyramidal axons by a continuous sinusoidal stimulation.

B. Volume Conductor Model

The induced scalar potential and EF were solved numerically by the scalar potential finite difference (SPFD [6]) carried out by Nagoya Institute of Technology and the finite element method (FEM) with rectilinear elements using Sim4Life software carried out by Ghent University [7]. These are based on the magneto-quasistatic methods. The computed induced EF and scalar electric potential corresponded to temporal peak values that were 2.65 times the EF computed at 10 kHz [8].

C. Pyramidal Axon Model

Activation thresholds of thick pyramidal axons were obtained for axons projected from the precentral gyrus of the hand motor area. The activation threshold is the lowest stimulation intensity necessary to propagate an action potential for each fast-conducting thickly myelinated pyramidal fibers (10 μm in diameter [9]). The axon of a myelinated neuron consists of internodes (segments ensheathed by myelin) and nodes of Ranvier (ionic channels). At the nodes of Ranvier, the ionic membrane current depends on the dynamics of voltage-gated sodium and leakage channels in the nodes, which is formulated as a conductance-based voltage-gated model. In this study, the Chiu-Ritchie-Rogart-Stagg-Sweeney (CRRSS) model was used [10]. The TMS-induced EF was coupled with the axon model. At the myelinated internodes, the leak conductance was modeled as a passive element or set to zero. The CRRSS model was implemented independently by two research groups: Nagoya Institute of Technology (Nitech [11]) and Ghent University (SENN-M and SENN-MA, where MA stands for myelin approximation) [12]. The Nitech and SENN-M models used the same parameters, while the SENN-MA implementation neglected the myelin capacitance and conductance. The set of model parameters used by each group

is summarized in table 1A (appendix). The elicitation of an action potential was indicated by the depolarization of the transmembrane potential by 50 mV, in at least four consecutive nodes of Ranvier using an in-house code

D. Data Analysis

The highest *in-situ* EFs values were suppressed because of numerical artifacts arising from stair-case approximation in voxelized models. The post-processing metrics to suppress the artifacts were 99.9th percentile, 99th percentile, and $2 \times 2 \times 2 \text{ mm}^3$ [2] in the brain (8×10^6 voxels). In the case of a 2-mm cube, the induced EF was averaged over 64 voxels. The Intercomparison between different implementations of the CRRSS models was quantified by the relative percentage difference of the activation thresholds $200|Th_1 - Th_2|/(Th_1 + Th_2)$.

III. NUMERICAL RESULTS

A. In-situ EF Intercomparison

Fig. 1 shows computed results for the *in-situ* field strength on the brain cortex during TMS stimulation over the CZ site. Similar EF distributions were obtained for the two numerical methods employed (SPFD and FEM). The voxel maximum of an *in-situ* EF is affected by the stair-casing error, as shown in Table 1. The volume-averaged (2-mm cube) value of the maximum EF provides some suppression when compared to the original resolution of 0.5 mm. The *in-situ* field strength values show less variation (around 59 mV/m) between the two numerical methods using the metrics of 99.9th percentile and 2-mm cube adapting 99.9th percentile. The maximum field strength at 1 mm and 2 mm inside the cortical surface (regions where thick pyramidal axons are projected from the grey matter) is larger than 99.9th percentile.

B. Nerve modelling Intercomparison

Intercomparison of the pyramidal axon activation is conducted in the motor hand area (Fig. 2). Independent implementations of the CRRSS model are compared in Figs. 3 using 63 fibers. The stimulation thresholds correspond to the *in-situ* EF strength or the external magnetic field. There is good agreement between the Nitech and SENN-M implementations and significant disagreement between Nitech and SENN-MA, as

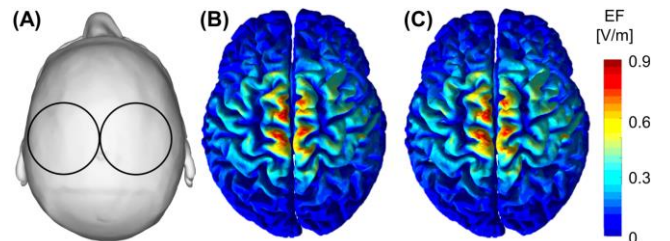


Fig. 1 Intercomparison of the *in-situ* EF in the brain cortex. (A) TMS coil is applied on the scalp on the Cz position. Computation is performed by (B) SPFD and (C) FEM numerical methods.

TABLE I. COMPUTED EF STRENGTH IN THE GRAY MATTER DURING TMS. 99.9TH PERCENTILE AND 99TH PERCENTILE ARE APPLIED FOR COMPUTED *IN-SITU* EF. ALSO, THE FIELD STRENGTH IS AVERAGED OVER 2×2×2 MM³ CUBE.

Metric	Numerical Methods	
	SPFD [mV/m]	FEM [mV/m]
Maximum	93.2	3368.4
2-mm Cube 99.9%ile	76.2	122.8
99.9% ile	61.6	61.2
2-mm Cube 99.9%ile	58.0	56.1
99 % ile	37.7	37.8
2-mm Cube 99 %ile	36.5	35.8
1 mm-depth	83.6	106.7
2 mm-depth	74.4	99.9

shown in Figs. 3a and 3b. The mean relative difference is 9.8% between Nitech and SENN-M. The variability of the relative difference is larger between Nitech and SENN-MA with a mean difference of 64.6%.

C. Reference Level

Threshold-frequency curves were derived from uniform exposure of the axons nerves in Fig. 2b and compared with current exposure limits issued by ICNIRP and IEEE. Fig. 4 shows that allowable external magnetic field strength and *in-situ* EF in the current guidelines/standard are conservative. Over the frequency range, IEEE reference level is conservative by factors of 5–60 and 9–31 for the *in-situ* EF and external magnetic field, respectively in a controlled environment. ICNIRP occupational basic restrictions are more conservative by factors of 15–67 and 64–261 for the *in-situ* EF and external magnetic field, respectively. The higher and lower factors are for 1 kHz and 100 kHz, respectively.

IV. DISCUSSION

This study investigated brain stimulation threshold variability by combined modelling of electromagnetics and neuron models for TMS. The computation of *in-situ* EF is corroborated by two different methods (SPFD and FEM), and intercomparison of pyramidal axons modelling results was conducted.

The voxel maximum of an *in-situ* EF is affected by the stair-casing error is inherent when using voxelized anatomical models [13]. This issue is listed in the research agenda of the IEEE International Committee on Electromagnetic Safety (ICES) [3]. In the case of TMS, suppression of numerical artifacts needs to be revised on the grey matter as the artifacts are more significant in comparison with the other head tissues due to the high conductivity contrast with cerebrospinal fluid. Analytical solutions existing for multi-spherical models of the head tissues have shown that suppression of numerical artifacts by using the 99.9th percentile method is effective for grey matter tissue [14]. However, computation of TMS-induced EFs is challenging because no analytical solutions exist for anatomical head models. As indirect verification, our results

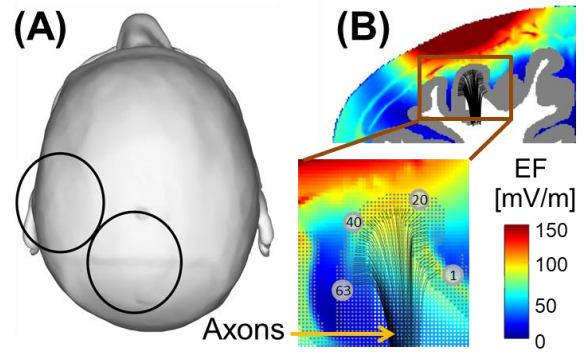


Fig. 2 (A) TMS exposure over the hand motor hand (B) Activation of sixty-three fibers projecting from the motor hand.

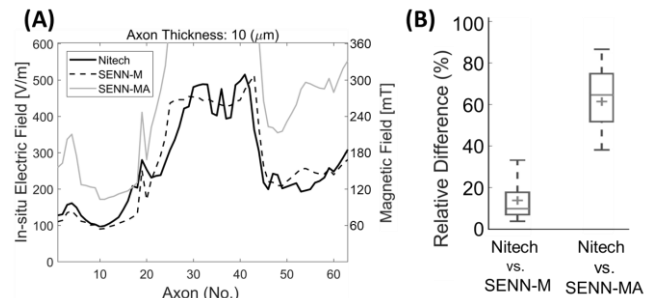


Fig. 3 (A) Intercomparison of pyramidal axon activation for fibers thickness of 10 μm . The axon numeration corresponds to Fig. 2B. (B) Relative percentage difference of the activation threshold.

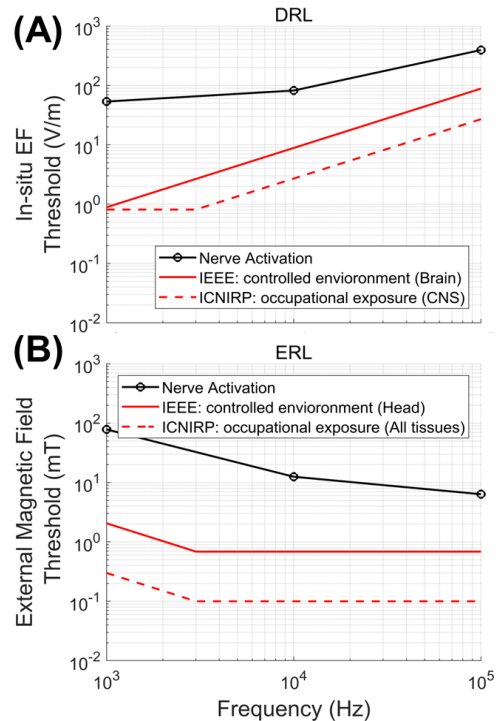


Fig. 4 Excitation thresholds for uniform exposure compared with ICNIRP guidelines and IEEE safety standard. (A) Dosimetry reference level. (B) Exposure reference level. Minimum threshold was selected between nerves in Fig. 2B (No. 11 to 60 with steps of 7) for each frequency.

confirmed that 99.9th percentile also is stable for two different numerical methods (SPFD and FEM), as shown in Table I. The 99th percentile would be a too conservative value considering that the field strength 2 mm below the cortical surface metric (Table 1) is two times higher.

Intercomparison of TMS-induced EF activation was conducted on fast-conducting thickly myelinated pyramidal fibers for corticospinal tracts (Betz cell's axon). The results showed that the *in-situ* EF (99.9th percentile) on the gray matter of the hand motor area was between 100 V/m and 200 V/m for activating axons with lower thresholds, which agrees with an estimated field for generating motor evoked potentials during TMS [15]. The external coil magnetic field was lower than 0.3 T which is lower than the maximum generated by a TMS device (1.5 T). Intercomparison showed that the excitation threshold agrees for independent implementations of the CRRSS model (9.8% of the relative difference in a group of axons). However, the selection of different model parameters (Ranvier node length, axoplasmatic resistivity, and membrane capacitance) has a six-fold increase of the relative difference of the stimulation threshold (Fig. 3). Sensitivity variation was less significant to myelin representation. The difference may be due to more sensitive variations of the electric potential along bent axon of large fibers.

The derived reference level in Fig. 4 showed that allowable external magnetic field strength and *in-situ* EF established by both guidelines/standards are significantly lower than the internal EF needed for the stimulation of the central nervous system for medical applications [16].

V. CONCLUSION

Intercomparison of electrostimulation threshold was conducted for a multiphysics model of TMS for the first time. A significant variation of the stimulation threshold was presented due to different morphological and electrical parameters selected in the axon model. However, the results showed that the relative difference was 10% between independent implementations of the CRRSS model with similar parameters. Reference levels defined by ICNIRP and IEEE international guidelines/standards were significantly conservative for nerve stimulation in the motor cortex of one subject during uniform exposure in the lateral–medial direction.

APPENDIX

The detailed implementation of the CRRSS model can be found in [11] for Nitech model and [12] for SENN-M and SENN-MA models. The parameters used by the two research groups are summarized in table A1.

Table A1. Nerve model parameters

Parameter	Nitech	SENN-M	SENN-MA
Inner diameter	0.64D ^a	0.64D	0.7D
Ranvier node length	1.5×10 ⁻⁴	1.5×10 ⁻⁴	2.5×10 ⁻⁴
No. of myelin layers	75×10 ⁴ D	75×10 ⁴ D	0
Axoplasmatic resistivity	0.07	0.07	0.11

Parameter	Nitech	SENN-M	SENN-MA
Myelin conductance/layer	1	1	0
Membrane capacitance	1	1	2.5

^a D is the external axon diameter

REFERENCES

- [1] IEEE, *IEEE standard for safety levels with respect to human exposure to electromagnetic fields, 0-3kHz*. Institute of Electrical and Electronics Engineers, 2002.
- [2] ICNIRP, "Guidelines for limiting exposure to time-varying electric, magnetic, and electromagnetic fields (up to 300 GHz). International Commission on Non-Ionizing Radiation Protection," *Health Phys.*, vol. 74, no. 4, pp. 494–522, Apr. 1998.
- [3] J. P. Reilly and A. Hirata, "Low-frequency electrical dosimetry: research agenda of the IEEE International Committee on Electromagnetic Safety," *Phys. Med. Biol.*, vol. 61, no. 12, pp. R138–R149, Jun. 2016.
- [4] R. Leo and T. Latif, "Repetitive Transcranial Magnetic Stimulation (rTMS) in Experimentally Induced and Chronic Neuropathic Pain: A Review," *J. Pain*, vol. 8, no. 6, pp. 453–459, Jun. 2007.
- [5] S. Gabriel, R. W. Lau, and C. Gabriel, "The dielectric properties of biological tissues: III. Parametric models for the dielectric spectrum of tissues," *Phys. Med. Biol.*, vol. 41, no. 11, p. 2271, Nov. 1996.
- [6] T. Dawson and M. Stuchly, "Analytic validation of a three-dimensional scalar-potential finite-difference code for low-frequency magnetic induction," *Appl. Comput. Electromagn. Soc. J.*, vol. 11, pp. 72–81, 1996.
- [7] E. Neufeld, D. Szczerba, N. Chavannes, and N. Kuster, "A novel medical image data-based multi-physics simulation platform for computational life sciences," *Interface Focus*, vol. 3, no. 2, p. 20120058, Apr. 2013.
- [8] B. D. Goodwin and C. R. Butson, "Subject-Specific Multiscale Modeling to Investigate Effects of Transcranial Magnetic Stimulation," *Neuromodulation Technol. Neural Interface*, vol. 18, no. 8, pp. 694–704, Dec. 2015.
- [9] L. Firmin, P. Field, M. A. Maier, A. Kraskov, P. A. Kirkwood, K. Nakajima, R. N. Lemon, and M. Glickstein, "Axon diameters and conduction velocities in the macaque pyramidal tract," *J. Neurophysiol.*, vol. 112, no. 6, pp. 1229–1240, 2014.
- [10] J. D. Sweeney, J. T. Mortimer, and D. Durand, "Modeling of mammalian myelinated nerve for functional neuromuscular electrostimulation," *IEEE 97th Annu. Conf. Eng. Med. Biol. Soc. Bost.*, vol. 9, pp. 1577–1578, 1987.
- [11] J. Gomez-Tames, T. Kutsuna, M. Tamura, Y. Muragaki, and A. Hirata, "Intraoperative direct subcortical stimulation: comparison of monopolar and bipolar stimulation," *Phys. Med. Biol.*, vol. 63, no. 22, p. 225013, Nov. 2018.
- [12] T. Tarnaud, W. Joseph, L. Martens, and E. Tanghe, "Dependence of excitability indices on membrane channel dynamics, myelin impedance, electrode location and stimulus waveforms in myelinated and unmyelinated fibre models," *Med. Biol. Eng. Comput.*, vol. 56, no. 9, pp. 1595–1613, Sep. 2018.
- [13] I. Laakso and A. Hirata, "Reducing the staircasing error in computational dosimetry of low-frequency electromagnetic fields," *Phys. Med. Biol.*, vol. 57, no. 4, pp. N25–N34, Feb. 2012.
- [14] J. Gomez-Tames, I. Laakso, Y. Haba, A. Hirata, D. Poljak, and K. Yamazaki, "Computational Artifacts of the In Situ Electric Field in Anatomical Models Exposed to Low-Frequency Magnetic Field," *IEEE Trans. Electromagn. Compat.*, pp. 1–9, 2017.
- [15] L. G. Cohen, B. J. Roth, J. Nilsson, N. Dang, M. Panizza, S. Bandinelli, W. Friauf, and M. Hallett, "Effects of coil design on delivery of focal magnetic stimulation. Technical considerations," *Electroencephalogr. Clin. Neurophysiol.*, vol. 75, no. 4, pp. 350–357, 1990.
- [16] M. Soldati, M. Mikkonen, I. Laakso, T. Murakami, Y. Ugawa, and A. Hirata, "A multi-scale computational approach based on TMS experiments for the assessment of electro-stimulation thresholds of the brain at intermediate frequencies," *Phys. Med. Biol.*, vol. 63, no. 22, p. 225006, Nov. 2018.